Electrostatic Caging

DOI: 10.1002/anie.201201627

Temporary Electrostatic Impairment of DNA Recognition: Light-Driven DNA Binding of Peptide Dimers**

Adrián Jiménez-Balsa, Elena Pazos, Borja Martínez-Albardonedo, José L. Mascareñas, and M. Eugenio Vázquez**

Dedicated to Professor Miguel Ángel Miranda on the occasion of his 60th birthday

Gene expression relies on a myriad of carefully orchestrated interactions between specialized proteins called transcription factors (TFs) and regulatory DNA sequences.[1] In general, such interactions are subtly regulated in time and space, so that many TFs remain inactive until receiving an appropriate activation signal.[2] It is well-established that the DNA readout by TFs largely relies on interactions between amino acid side chains and the DNA bases and phosphates.[3] Among these contacts, those involving positively charged basic amino acids are critical for the thermodynamic stability of their DNA complexes.[4] We reasoned that the temporary electrostatic deactivation of such contacts might provide for the development of TF-based systems where DNA binding activity could be externally controllable, for instance by light. These systems could be useful methods for transcriptional control,[5] or for probing spatiotemporal patterns of gene expression in living organisms.[6] It is curious that despite the well-established use of light-activated compounds in chemical biology,[7,8] examples of photocontrolled DNA binding are certainly scarce. These include reversible switches based on the photostationary equilibrium of azo-modified DNA binders,[5,9] special chromophores with poor DNA binding affinity and/or specificity,[10] and single-use caging strategies for triggering minor groove binding or intercalation.[11] Thus, inspired by the use of negatively charged elements to modulate cell internalization,[12] we sought to develop a general strategy for photocontrolling the sequence-specific DNA binding of TF peptide mimics.

Herein we demonstrate that tethering polyanionic tails to basic DNA-binding bZIP peptides through a light-sensitive linker suppresses the DNA interaction. Upon irradiation, the negatively charged appendages are released, and the DNA-binding activity is thus restored. As reference system for implementing the strategy we chose the GCN4 transcription factor, an archetypical bZIP TF that specifically binds to ATF/CREB (5′-ATGA(c/g)TCAT-3′) or AP1 (5′-ATGA(c)TCAT-3′) sites as a leucine zipper-mediated dimer of uninterrupted α helices. The N-terminal basic regions feature many positively charged amino acids that are key for the DNA recognition (10 Lys or Arg out of 31 residues in the basic region; Figure 1, GCN4br).[13] It has been shown that the leucine zipper itself can be substituted by a number of dimerizing units without significant loss in the DNA binding properties.[14] Therefore, in our first iteration for the design of the electrostatically impaired DNA-binding peptides, we selected the minimum sequence of the bZIP basic region (br) that it is known to retain the DNA binding ability when engineered as a disulfide dimer.[15] This minimal peptide was extended at the N-terminus by adding acidic extensions with four or eight Glu residues linked to the core br sequence

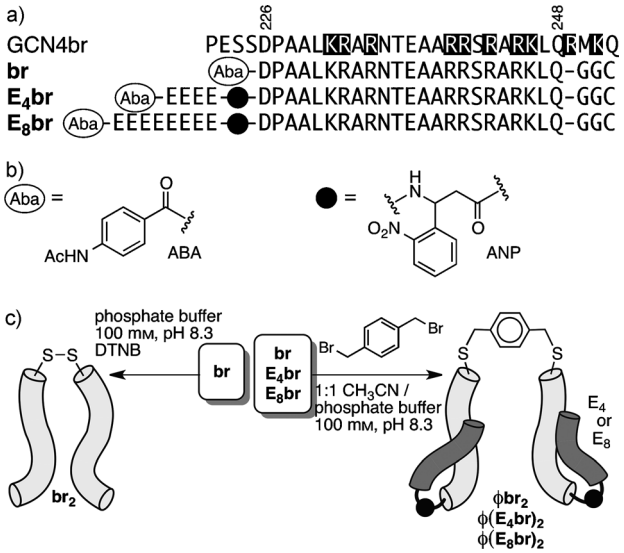

Figure 1. a) Sequence of the GCN4 basic region highlighting the positively charged residues. Sequences of peptides with acidic tails, E_4br and E_8br. b) Structure of the Aba chromophore (used as internal standard), and the ANP photocleavable linker (shown as ●). c) Dimerization reactions of br, E_4br, and E_8br to give the corresponding control disulfide br_2, or benzylic dimers, ϕbr_2, $\phi(E_4br)_2$, and $\phi(E_8br)_2$. The acidic tails (Glu_4 or Glu_8) are represented by darker gray and the photocleavable element as a black circle.

[*] A. Jiménez-Balsa, Dr. E. Pazos, B. Martínez-Albardonedo, Prof. J. L. Mascareñas, Prof. M. E. Vázquez
Departamento de Química Orgánica y Centro Singular de Investigación en Química Biológica y Materiales Moleculares y Unidad Asociada al CSIC, Universidade de Santiago de Compostela
15782 Santiago de Compostela (Spain)
E-mail: joseluis.mascarenas@usc.es
eugenio.vazquez@usc.es
Homepage: http://www.usc.es/chembiousc/

[**] We thank the financial support provided by the Spanish grants SAF2010-20822-C02, CTQ2009-14431/BQU, Consolider Ingenio 2010 CSD2007-00006, and the Xunta de Galicia INCITE09 209 084PR, PGIDIT08CSA-047209PR, and GRC2010/12. A.J.B. and E.P. thank the Spanish MINECO and the Xunta for their PhD fellowships.

Supporting information for this article is available on the WWW under http://dx.doi.org/10.1002/anie.201201627.

through a photolabile 3-amino-3-(2-nitrophenyl)propionic acid (ANP) group.[16] The disulfide control peptide br_2 was constructed by dimerization of the monomers containing a C-terminal cysteine by using Ellman's reagent in phosphate buffer.[17] Peptide dimers $\phi(br)_2$, $\phi(E_4br)_2$, and $\phi(E_8br)_2$ were obtained in good yield by direct alkylation of each of the cystein monomers with 1,4-bis(bromomethyl)benzene.

The DNA binding of ϕbr_2, $\phi(E_4br)_2$, and $\phi(E_8br)_2$ was studied by electrophoretic mobility shift assays (EMSA) under non-denaturing conditions[18] and using SYBR gold for DNA staining. Thus, a short ds oligonucleotide containing the ATF/CREB binding site was incubated with each of the three peptides at 4 °C. As a positive binding control, we used the basic region disulfide dimer br_2, which in the presence of the ATF/CREB oligo gave the expected slower migrating band (Figure 2, lanes 2–4, band b). The ϕbr_2 dimer displayed

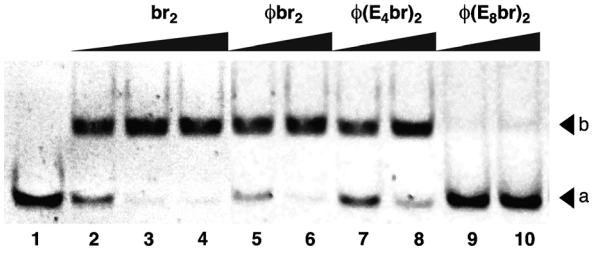

Figure 2. EMSA assays of DNA recognition. Lanes 1–10: target ATF/CREB dsDNA (50 nM). Lanes 2–4: 75, 150, 300 nM br_2; lanes 5, 6: 150, 300 nM ϕbr_2; lanes 7, 8: 150, 300 nM $\phi(E_4br)_2$; lanes 9, 10: 150, 300 nM $\phi(E_8br)_2$. Band (a) corresponds to the free ds-oligo; the slow-migrating band (b) corresponds to the DNA/peptide complexes.[19] ATF/CREB (one strand shown, binding site in italics): 5′-TGGAG *AT-GA* cg *TCAT* CTCGT-3′. Peptide and dsDNA in 5 mM Tris-HCl, pH 6.8, 50 mM NaCl, (4 °C, 10 min) were added to 18 mM Tris-HCl pH 7.5, 90 mM KCl, 1.8 mM $MgCl_2$, 1.8 mM EDTA, 9% glycerol, 0.11 mg mL^{-1} BSA, 2.25% NP-40 (4 °C, 10 min) and loaded into the gel.

qualitatively similar binding properties as the positive control, albeit exhibiting a slightly reduced affinity (Figure 2, lanes 5 and 6). Curiously, the dimer $\phi(E_4br)_2$ also displayed measurable affinity for the target oligonucleotide, despite the presence of a significant number of negatives charges (two Glu_4 tails), as evidenced by the appearance of a retarded band in the gel similar that observed with the controls (Figure 2, lanes 7 and 8). In contrast, the $\phi(E_8br)_2$ peptide, featuring the longer Glu_8 acidic tails, was incapable of forming stable complexes in the electrophoretic gel, and only at high peptide concentrations it was possible to observe a faint, slower migrating band (lanes 9 and 10).

Once we had confirmed that the Glu_8 acidic appendages significantly impaired the DNA binding, we investigated the photocleavage of the ANP linker. Unfortunately, HPLC analysis of the irradiated solution of $\phi(E_8br)_2$ (30 s, $\lambda = 300$–375 nm) showed a complex mixture of products that could not be characterized (Figure 3a) and from which it was not possible to isolate the expected photocleaved dimer. Addition of commonly used reagents to capture reactive photolysis byproducts, such as DTT or hydrazine,[20] did not result in any significant improvement. Considering that the complex product mixture could arise from the degradation of highly

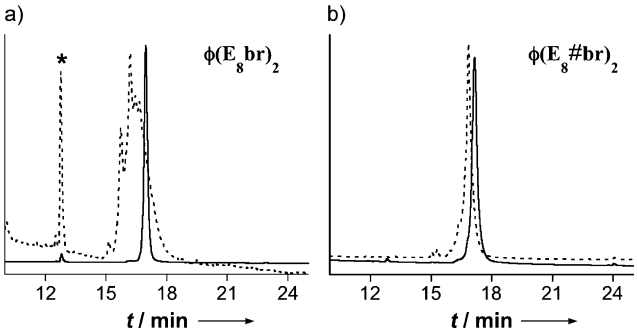

Figure 3. HPLC traces of the irradiated buffered solutions of a) $\phi(E_8br)_2$ and b) $\phi(E_8\#br)_2$, showing the improved photolysis in the reversed design (5 to 75%, 0.1% TFA CH_3CN/H_2O). —— Starting dimers, ----- chromatograms after 30 s irradiation. The acidic tail released upon irradiation of $\phi(E_8br)_2$ is marked with an asterisk. The major peak in the trace at the right corresponds to the expected uncaged dimer $\phi(Q\#br)_2$. The photoreleased acidic tail containing the reactive nitrosoketone group is not observed in this case, probably because it decomposes and the degraded products are eluted with the injection peak; traces of the dimer with one acidic tail were also observed in the MALDI spectra (see the Supporting Information).

reactive phenylnitroso ketone groups photoreleased at the N-terminus of the active peptide fragments, we modified the design, reversing the orientation of the ANP linker.[21] The new $\phi(E_8\#br)_2$ peptide contained a reconfigured ANP linker attached to the side chain of a Glu residue at the N-terminus of the basic region; cleavage of this inverted ANP would release the intact native peptide, leaving a natural Gln residue at the N-terminus ($\phi(Q\#br)_2$; Scheme 1).

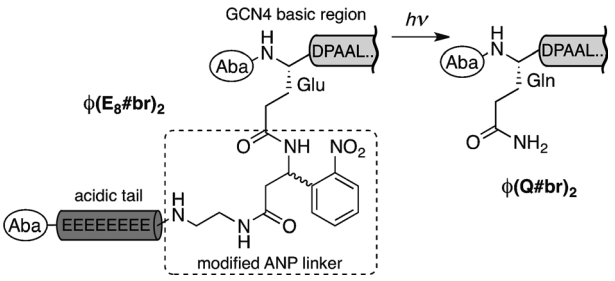

Scheme 1. Structure of the modified photolabile basic regions with the reversed ANP linker connected through a Glu side chain ($\phi(E_8\#br)_2$), and the expected photodissociation product, $\phi(Q\#br)_2$.

The revamped $\phi(E_8\#br)_2$ peptide was synthesized following a similar procedure to that described previously for the synthesis of $\phi(E_8br)_2$. Gratifyingly, we found that photolysis of $\phi(E_8\#br)_2$ was much cleaner than that of $\phi(E_8br)_2$, as shown by the HPLC analysis of the reaction mixture (Figure 3; Supporting Information).

As expected, the inverted peptide $\phi(E_8\#br)_2$ qualitatively reproduces the DNA-binding behavior observed with the original $\phi(E_8br)_2$ peptide. Thus incubation of $\phi(E_8\#br)_2$ with a double stranded oligonucleotide containing the ATF/CREB target sequence did not show significant retarded bands in the PAGE experiments (Figure 4a, lanes 2–5). Irradiation of a 50 μM solution of $\phi(E_8\#br)_2$ in 10 mM Tris-HCl pH 6.8

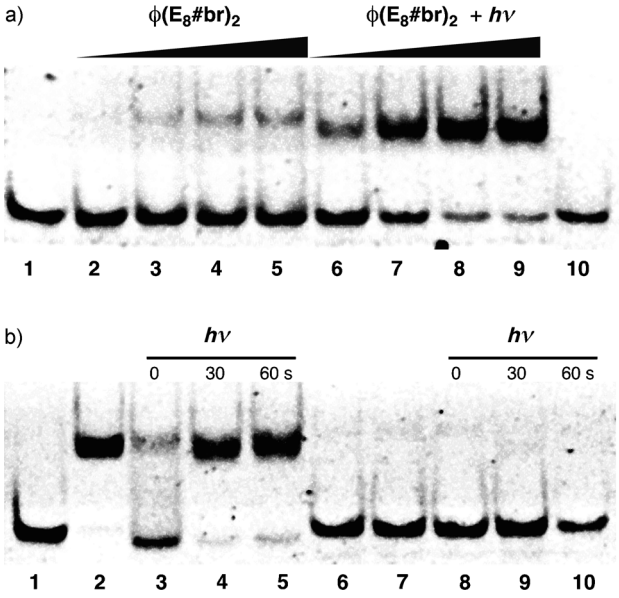

Figure 4. EMSA analysis of DNA binding by $\phi(E_8\#br)_2$ at 4 °C. a) Lanes 1–9: target ATF/CREB oligo (50 nM). Lanes 2–5: 125, 250, 400, 600 nM $\phi(E_8\#br)_2$, no irradiation; lanes 6–9: 125, 250, 400, 600 nM $\phi(E_8\#br)_2$, after 30 s irradiation with UV light (10 mM Tris-HCl, pH 6.8); lane 10: 600 nM $\phi(E_8\#br)_2$ after 30 s irradiation and addition of a random ds-oligo (*rnd*DNA, 50 nM; see the Supporting Information for the full sequence). b) DNA binding of $\phi(E_8\#br)_2$; irradiation in the presence of the oligonucleotide (10 mM Tris-HCl, pH 6.8). Lanes 1–5: target ATF/CREB oligo (50 nM). Lane 2: control peptide ϕbr_2 (300 nM). Lanes 3–5: $\phi(E_8\#br)_2$ (300 nM) at increased irradiation times; lanes 6–10: *rnd*DNA (50 nM); lane 7: control, ϕbr_2 (300 nM); lanes 8–10: $\phi(E_8\#br)_2$ (300 nM) at increasing irradiation times.

It is well-known that the DNA binding of bZIP dimers is coupled to their folding into α-helical conformations.[23] Therefore we carried out complementary circular dichroism studies to gain some structural insight into the DNA binding process. These experiments showed that the caged dimer $\phi(E_8\#br)_2$ is essentially unstructured in the absence of DNA (Figure 5a, open circles). Addition of the target ATF/CREB

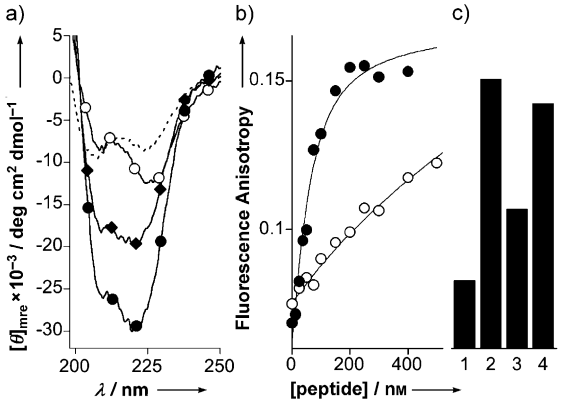

Figure 5. a) CD spectra of 5 μM $\phi(E_8\#br)_2$ in 10 mM Tris-HCl, pH 6.8, at 4 °C (-----). —— $\phi(E_8\#br)_2$ after 30 s irradiation (○); $\phi(E_8\#br)_2$ in the presence of 5 μM of the target oligo ATF/CREB before (◆), and after 30 s irradiation (●). b) Fluorescence anisotropy titrations at 518 nm of a fluorescein-labeled ATF/CREB (50 nM) with $\phi(E_8\#br)_2$ (○), with the $\phi(Q\#br)_2$ control (●), and best fit to a simple 1:1 binding model (10 mM Tris-HCl buffer, 10 mM NaCl, pH 6.8 at 10 °C). c) Fluorescence anisotropy values: oligo ATF/CREB (50 nM) (bar 1); oligo with 300 nM $\phi(Q\#br)_2$ (bar 2); same oligo with 300 nM $\phi(E_8\#br)_2$ (bar 3); and with 300 nM $\phi(E_8\#br)_2$ after 60 s irradiation (bar 4). The same scale is used as with the titrations.

buffer for 30 s with a standard gel transilluminator lamp, and subsequent incubation with the same oligonucleotide, resulted in the appearance of retarded gel bands, which is consistent with a specific peptide–DNA complex (Figure 4a, lanes 6–9).[22] Moreover, these bands were similar to those observed using the $\phi(Q\#br)_2$ peptide dimer, which was purposely synthesized de novo as a true uncaged control. As expected, incubation of the irradiated sample of $\phi(E_8\#br)_2$ with a random DNA did not result in any new band (Figure 4a, lane 10). Along with the experiments with the symmetrically caged $\phi(E_8\#br)_2$, we synthesized a single-caged $\phi(Q\#br)(E_8\#br)$ peptide in which only one of the basic regions was modified with the acidic tail. Remarkably, this peptide retained a significant DNA binding affinity, showing in the EMSA gels as a slightly slower migrating band than that of the complex with the uncaged control $\phi(Q\#br)_2$ (Supporting Information, Figure S17).

Importantly, the photochemical activation can be carried out in the presence of the DNA. Therefore, irradiating a mixture of $\phi(E_8\#br)_2$ and the target oligonucleotide allowed a substantial recovery of the DNA binding, as shown by EMSA (Figure 4b, lanes 3–5). An irradiation control experiment with a random oligonucleotide confirmed the specificity of the interaction, as in this case we did not observe the formation of new retarded bands in the gel (Figure 4b, lanes 8–10).

oligonucleotide induced a significant increase in the negative CD signal at 222 nm, which is consistent with an increase in the α-helical content of the peptide that could result from the high concentrations required to run the CD experiments (5 μM of peptide and DNA), or from nonspecific interactions with the dsDNAs.[24] More importantly, UV irradiation of this $\phi(E_8\#br)_2$/oligonucleotide mixture led to a large increase in the negative ellipticity in the range of what has been observed when this type of dimers fold upon interacting with their target DNA sites (Figure 5a).[23]

To further confirm these results and rule out any distortions associated with the gel shift experiments, we performed fluorescence anisotropy titrations that provided a more quantitative characterization of the DNA recognition process.[25] Incubation of a fluorescein-labeled ATF/CREB oligonucleotide with increasing amounts of $\phi(Q\#br)_2$ resulted in a progressive increase of the anisotropy, which was consistent with the formation of a DNA complex with higher molecular weight and reduced mobility.[26] Fitting of the resulting isotherm to a 1:1 binding model,[27] allowed to calculate its dissociation constant ($K_D \approx 38$ nM). As expected, the caged derivative $\phi(E_8\#br)_2$ showed drastically weaker binding than the control peptide under the same conditions ($K_D \approx 1$ μM; Figure 5b, open circles). Moreover, the uncaging process could be monitored by fluorescence anisotropy. Thus,

irradiation of the caged $\phi(E_8\#br)_2$ peptide in the presence of the fluorescence-labeled ATF/CREB oligonucleotide resulted in an anisotropy value similar to that obtained when the target oligonucleotide is incubated with the $\phi(Q\#br)_2$ control peptide (Figure 5c).

In conclusion, we have demonstrated that the attachment of a negatively charged tether to an Arg/Lys-rich bZIP-based peptide can effectively hamper its DNA recognition ability. Moreover, connecting this appendage through a photocleavable ANP linker allows to restoring the DNA binding upon simple UV irradiation. The negatively charged patch might disturb the binding by interfering with electrostatic pairing or by generating repulsive contacts with the DNA. Typical photocaging or switching strategies are based on the modification of specific key residues and usually require linear synthetic processes as well as detailed structural knowledge of the interaction. Our electrostatic turn-off strategy, by relying on simple tethering of highly charged appendages to the natural recognition elements, should provide a facile, versatile, and general route to temporarily control specific biological interactions involving highly charged partners, such as nucleic acids. Furthermore, this method seems particularly appropriate for modulating interactions involving multivalent contacts that might tolerate a single caging group.

Received: February 29, 2012
Published online: July 31, 2012

Keywords: amino acids · DNA recognition · peptides · photochemistry · protein design

[1] D. S. Latchman, *Eukaryotic Transcription Factors*, Elsevier, London, **2004**.
[2] J. E. Darnell, Jr., *Nat. Rev. Cancer* **2002**, *2*, 740 – 749.
[3] C. W. Garvie, C. Wolberger, *Mol. Cell* **2001**, *8*, 937 – 946; Y. Choo, A. Klug, *Curr. Opin. Struct. Biol.* **1997**, *7*, 117 – 125; N. M. Luscombe, R. A. Laskowski, J. M. Thornton, *Nucleic Acids Res.* **2001**, *29*, 2860 – 2874; Y. Mandel-Gutfreund, O. Schueler, H. Margalit, *J. Mol. Biol.* **1995**, *253*, 370 – 382.
[4] T. Härd, T. Lundbäck, *Biophys. Chem.* **1996**, *62*, 121 – 139; J. Norberg, *Arch. Biochem. Biophys.* **2003**, *410*, 48 – 68; A. G. Cherstvy, *J. Phys. Chem. B* **2009**, *113*, 4242 – 4247; V. R. Ramirez-Carrozzi, T. K. Kerppola, *J. Mol. Biol.* **2001**, *305*, 411 – 427; C. O. Pabo, R. T. Sauer, *Annu. Rev. Biochem.* **1992**, *61*, 1053 – 1095.
[5] A. Nomura, A. Okamoto, *Chem. Commun.* **2009**, 1906 – 1908; F. Zhang, K. A. Timm, K. M. Arndt, G. A. Woolley, *Angew. Chem.* **2010**, *122*, 4035 – 4038; *Angew. Chem. Int. Ed.* **2010**, *49*, 3943 – 3946; S.-A. Morgan, M. S. Al-Abdul-Wahid, G. A. Woolley, *J. Mol. Biol.* **2010**, *399*, 94 – 112.
[6] S.-A. Morgan, G. A. Woolley, *Photochem. Photobiol. Sci.* **2010**, *9*, 1320 – 1326.
[7] R. Wieboldt, K. R. Gee, L. Niu, D. Ramesh, B. K. Carpenter, G. P. Hess, *Proc. Natl. Acad. Sci. USA* **1994**, *91*, 8752 – 8756; A. Nguyen, D. M. Rothman, J. Stehn, B. Imperiali, M. B. Yaffe, *Nat. Biotechnol.* **2004**, *22*, 993 – 1000; M. E. Vázquez, M. Nitz, J. Stehn, M. B. Yaffe, B. Imperiali, *J. Am. Chem. Soc.* **2003**, *125*, 10150 – 10151.
[8] H. Yu, J. Li, D. Wu, Z. Qiu, Y. Zhang, *Chem. Soc. Rev.* **2010**, *39*, 464 – 473; Y. Ohmuro-Matsuyama, Y. Tatsu, *Angew. Chem.* **2008**, *120*, 7637 – 7639; *Angew. Chem. Int. Ed.* **2008**, *47*, 7527 – 7529; A. Gautier, D. P. Nguyen, H. Lusic, W. An, A. Deiters, J. W. Chin, *J. Am. Chem. Soc.* **2010**, *132*, 4086 – 4088; D. Humphrey, Z. Rajfur, M. E. Vázquez, D. Scheswohl, M. D. Schaller, K. Jacobson, B. Imperiali, *J. Biol. Chem.* **2005**, *280*, 22091 – 22101.
[9] A. M. Caamaño, M. E. Vázquez, J. Martínez-Costas, L. Castedo, J. L. Mascareñas, *Angew. Chem.* **2000**, *112*, 3234 – 3237; *Angew. Chem. Int. Ed.* **2000**, *39*, 3104 – 3107; L. Guerrero, O. S. Smart, G. A. Woolley, R. K. Allemann, *J. Am. Chem. Soc.* **2005**, *127*, 15624 – 15629.
[10] J. Andersson, S. Li, P. Lincoln, J. Andréasson, *J. Am. Chem. Soc.* **2008**, *130*, 11836 – 11837; M. L. Di Pietro, F. Puntoriero, F. Tuyéras, P. Ochsenbein, P. P. Lainé, S. Campagna, *Chem. Commun.* **2010**, *46*, 5169 – 5171.
[11] M. I. Sánchez, O. Vázquez, M. E. Vázquez, J. L. Mascareñas, *Chem. Commun.* **2011**, *47*, 11107 – 11109; O. Vázquez, M. I. Sánchez, J. Martínez-Costas, M. E. Vázquez, J. L. Mascareñas, *Org. Lett.* **2010**, *12*, 216 – 219; M. I. Sánchez, J. Martínez-Costas, F. González, M. A. Bermúdez, M. E. Vázquez, J. L. Mascareñas, *ACS Chem. Biol.* **2012**, *7*, 1276 – 1280.
[12] E. S. Olson, T. A. Aguilera, T. Jiang, L. G. Ellies, Q. T. Nguyen, E. H. Wong, L. A. Gross, R. Y. Tsien, *Integrative Biol.* **2009**, *1*, 382 – 393; T. Jiang, E. S. Olson, Q. T. Nguyen, M. Roy, P. A. Jennings, R. Y. Tsien, *Proc. Natl. Acad. Sci. USA* **2004**, *101*, 17867 – 17872.
[13] T. E. Ellenberger, C. Brandl, K. Struhl, S. C. Harrison, *Cell* **1992**, *71*, 1223 – 1237; P. König, T. J. Richmond, *J. Mol. Biol.* **1993**, *233*, 139 – 154.
[14] E. Pazos, J. Mosquera, M. E. Vázquez, J. L. Mascareñas, *ChemBioChem* **2011**, *12*, 1958 – 1973; M. E. Vázquez, A. M. Caamaño, J. L. Mascareñas, *Chem. Soc. Rev.* **2003**, *32*, 338 – 349; M. E. Vázquez, A. M. Caamaño, J. Martínez-Costas, L. Castedo, J. L. Mascareñas, *Angew. Chem.* **2001**, *113*, 4859 – 4861; *Angew. Chem. Int. Ed.* **2001**, *40*, 4723 – 4725; S.-I. Sato, M. Hagihara, K. Sugimoto, T. Morii, *Chem. Eur. J.* **2002**, *8*, 5066 – 5071.
[15] R. V. Talanian, C. J. McKnight, R. Rutkowski, P. S. Kim, *Biochemistry* **1992**, *31*, 6871 – 6875; for other DNA-binding bZIP-based peptides, see: J. Blanco, M. E. Vázquez, J. Martínez-Costas, L. Castedo, J. L. Mascareñas, *Chem. Biol.* **2003**, *10*, 713 – 722; J. B. Blanco, O. Vázquez, J. Martínez-Costas, L. Castedo, J. L. Mascareñas, *Chem. Eur. J.* **2005**, *11*, 4171 – 4178; O. Vázquez, M. E. Vázquez, J. B. Blanco-Canosa, L. Castedo, J. L. Mascareñas, *Angew. Chem.* **2007**, *119*, 7010 – 7014; *Angew. Chem. Int. Ed.* **2007**, *46*, 6886 – 6890.
[16] C. Grunwald, K. Schulze, A. Reichel, V. U. Weiss, D. Blaas, J. Piehler, K.-H. Wiesmüller, R. Tampé, *Proc. Natl. Acad. Sci. USA* **2010**, *107*, 6146 – 6151; M. Nitz, K. J. Franz, R. L. Maglathlin, B. Imperiali, *ChemBioChem* **2003**, *4*, 272 – 276.
[17] See the Supporting Information. For this type of disulfide formation, see: G. T. Hermanson, *Bioconjugate Techniques*, Academic Press/Elsevier, London, **2008**; S. Arpicco, F. Dosio, P. Brusa, P. Crosasso, L. Cattel, *Bioconjugate Chem.* **1997**, *8*, 327 – 337.
[18] W. Hendrickson, *BioTechniques* **1985**, *3*, 346 – 354; A. Revzin, *BioTechniques* **1989**, *7*, 346 – 354; D. Lane, P. Prentki, M. Chanler, *Microbiol. Rev.* **1992**, *56*, 509 – 529; L. M. Hellman, M. G. Fried, *Nat. Protoc.* **2007**, *2*, 1849 – 1861.
[19] This figure is a composite of two independent experiments of br_2 and ϕbr_2 with $\phi(E_4Br)_2$ and $\phi(E_8Br)_2$.
[20] O. Ito, M. Matsuda, *Bull. Chem. Soc. Jpn.* **1978**, *51*, 427 – 430; O. Mozziconacci, V. Sharov, T. D. Williams, B. A. Kerwin, C. Schöneich, *J. Phys. Chem. B* **2008**, *112*, 9250 – 9257.
[21] C. J. Bosques, B. Imperiali, *J. Am. Chem. Soc.* **2003**, *125*, 7530 – 7531.
[22] The shift of this band is matches that of a specifically synthetized dimeric control peptide $\phi(Q\#br)_2$ (see the Supporting Information).
[23] R. V. Talanian, C. J. McKnight, P. S. Kim, *Science* **1990**, *249*, 769 – 771; Y. Aizawa, Y. Sugiura, T. Morii, *Biochemistry* **1999**, *38*,

1626 – 1632; G. Holzwarth, P. Doty, *J. Am. Chem. Soc.* **1965**, *87*, 218 – 228.

[24] Related structuring effects have been observed with positively charged peptides as a result of low affinity and non-specific interactions with DNA: A. Zlotnick, S. L. Brenner, *J. Mol. Biol.* **1988**, *209*, 447 – 457; K. Niikura, H. Matsuno, Y. Okahata, *Chem. Eur. J.* **1999**, *5*, 1609 – 1616; N. P. Johnson, J. Lindstrom, W. A. Baase, P. H. von Hippel, *Proc. Natl. Acad. Sci. USA* **1994**, *91*, 4840 – 4844.

[25] B. J. Anderson, C. Larkin, K. Guja, J. F. Schildbach, *Methods Enzymol.* **2008**, *450*, 253 – 272; G. H. Bird, A. R. Lajmi, J. A. Shin, *Biopolymers* **2002**, *65*, 10 – 20.

[26] V. J. LiCata, A. J. Wowor, *Methods Cell Biol.* **2008**, *84*, 243 – 262.

[27] J. R. Lundblad, M. Laurance, R. H. Goodman, *Mol. Endocrinol.* **1996**, *10*, 607 – 612. Experimental data were fitted with the *DynaFit 3* software. P. Kuzmič, *Anal. Biochem.* **1996**, *237*, 260 – 273.

